

VUV $5d-4f$ luminescence of Gd^{3+} and Lu^{3+} ions in the CaF_2 host

© V.N. Makhov^{*,**}, S.Kh. Batygov^{***}, L.N. Dmitruk^{***}, M. Kirm^{**}, S. Vielhauer^{**}, G. Stryganyuk^{****}

* P.N. Lebedev Physical Institute, Russian Academy of Sciences,
119991 Moscow, Russia

** Institute of Physics, University of Tartu,
51014 Tartu, Estonia

*** General Physics Institute, Russian Academy of Sciences,
119991 Moscow, Russia

**** Hamburger Synchrotronstrahlungslabor HASYLAB, Deutsches Elektronensynchrotron
DESY, 22607 Hamburg, Germany

E-mail: makhov@sci.lebedev.ru

First observation and characterization of $Lu^{3+} 4f^{13}5d-4f^{14}$ luminescence from the $CaF_2:Lu^{3+}$ crystal are reported, and the multi-site structure in the spectra of Ce^{3+} , Gd^{3+} and Lu^{3+} ions in the CaF_2 host is analyzed with the high-resolution VUV spectroscopy technique using synchrotron radiation. It was shown that vibronic structure in the emission and excitation spectra of interconfigurational transitions in Gd^{3+} and Lu^{3+} ions doped into CaF_2 differs from that observed for Ce^{3+} ions entering mainly at the tetragonal (C_{4v}) sites. However, the exact types of sites in which the Gd^{3+} and Lu^{3+} ions reside in the CaF_2 lattice cannot be identified basing only on obtained experimental spectroscopic data.

This work was supported by the RFBR Grant 05-02-1730, the Estonian Science Foundation Grant 6538 and the European Community Research Infrastructure Action within the FP6 Program through the Contract RII3-CT-2004-506008 (IA-SFS).

PACS: 78.55.Hx, 71.70.Ch, 63.20.Kr, 78.47.+p

1. Introduction

Trivalent rare earth (RE) ions incorporated into CaF_2 substitute for Ca^{2+} ions. The extra positive charge of the RE^{3+} ion relative to Ca^{2+} needs some mechanism of charge compensation. It is usually accepted that at doping concentration below $\sim 0.1\%$ the RE^{3+} ions of any kind reside in CaF_2 predominantly in the tetragonal C_{4v} sites where charge compensation of RE^{3+} is achieved by an interstitial fluorine ion located at the nearest-neighbor position along [100] direction from the RE^{3+} ion [1–3]. The vibronic structure in the spectra of interconfigurational $4f^n-4f^{n-1}5d$ transitions in most of RE^{3+} ions located at the tetragonal sites is dominated by the line at the energy interval $\sim 480\text{ cm}^{-1}$ from zero-phonon lines (ZPL). However, the RE^{3+} centers of different symmetry were also detected for many RE^{3+} ions [4–6]. In particular, the trigonal centers (C_{3v}) are observed, in which charge compensation is achieved by the fluorine ion in the next-nearest neighbor position along [111] direction from the RE^{3+} ion (if the crystals were grown under reducing conditions). The cubic (O_h) centers with remote charge compensation by mono-valent impurity ions, e.g. by doping with Na^+ or Li^+ , were also identified [7,8].

Recent studies [9–13] have revealed that several Gd^{3+} and Lu^{3+} containing fluoride crystals with sufficiently wide band-gap emit luminescence in the deep vacuum ultraviolet (VUV) spectral range ($h\nu \sim 10\text{ eV}$), which is due to the interconfigurational $4f^65d-4f^7$ transitions in the Gd^{3+} ion and $4f^{13}5d-4f^{14}$ transitions in the Lu^{3+} ion. In the case of crystals with scheelite ($LiYF_4$) or YF_3 structure, the Gd^{3+} and Lu^{3+} ions substitute for the Y^{3+} ions almost

without distortion of the crystal lattice. As a result, the vibronic structure in the spectra of different RE^{3+} ions looks very similar, being determined by the phonon spectrum of the host lattice. In particular, the fine structure of the $Gd^{3+} 4f^65d-4f^7$ emission spectrum almost coincide in shape with that of the $Ce^{3+} 4f-5d$ excitation (absorption) spectrum for $LiGdF_4:Ce^{3+}$ crystal [12]. On the other hand, it was found that vibronic structure in emission and excitation spectra of $Gd^{3+}4f^65d-4f^7$ luminescence from the $CaF_2:Gd^{3+}$, Ce^{3+} crystal [13] differs significantly from that observed for other trivalent RE ions doped into CaF_2 , similar to earlier observations in the $Gd^{3+} 4f^7-4f^65d$ absorption spectrum of $CaF_2:Gd^{3+}$ [14]. In the present work, the $Lu^{3+} 4f^{13}5d-4f^{14}$ luminescence from the $CaF_2:Lu^{3+}$, Ce^{3+} crystal has been detected, assigned and characterized, and the multi-site structure in the spectra of Ce^{3+} , Gd^{3+} and Lu^{3+} ions in the CaF_2 host has been analyzed using the high-resolution VUV spectroscopy technique.

2. Experimental details

High-resolution emission and excitation spectra have been measured using the SUPERLUMI set-up operated at the DORIS storage ring of HASYLAB at DESY [15–16]. VUV emission spectra were recorded using an open position sensitive microchannel-plate detector coated with CsI in combination with a 1 m VUV monochromator, at resolutions up to 0.5 \AA in second order. The excitation spectra of VUV emission were recorded using a Pouey type monochromator (typical spectral resolution $\Delta\lambda=20\text{ \AA}$) equipped with a CsI

sensitized microsphere plate detector. A 0.3 m Czerny-Turner-type monochromator-spectrograph SpectraPro-308i (Acton Research Inc.) with a R6358P (Hamamatsu) photomultiplier tube was applied for measuring excitation spectra of UV/visible luminescence. Emission spectra in the UV/visible spectral range were recorded at the same spectrograph SpectraPro-308i with a liquid nitrogen cooled CCD detector (Princeton Instruments Inc.). The spectral resolution of ~ 0.2 nm was achieved with the 1200 grooves/mm grating using 0.05 mm slit width. The excitation spectra were recorded with an instrumental resolution of primary monochromator as high as 0.7 \AA . The wavelength positions of all features in VUV emission and excitation spectra were determined with accuracy of $\sim 0.5 \text{ \AA}$.

Single crystals of CaF_2 singly doped with 0.1 mol.% Ce^{3+} , doubly doped with 0.1 mol.% Gd^{3+} and 0.05 mol.% Ce^{3+} and doubly doped with 0.04 mol.% Lu^{3+} and 0.02 mol.% Ce^{3+} were grown by the vertical Bridgman method in the fluorine atmosphere. The samples were cleaved prior to the mounting onto a copper sample holder attached to cold finger of a flow-type liquid helium cryostat (Cryovac GmbH).

3. Results and discussion

Fast ($\tau \sim 8.5$ ns) VUV luminescence is observed from the Gd^{3+} doped CaF_2 crystals, which is due to $4f^{65d}-4f^7$ radiative transitions in Gd^{3+} (Fig. 1) [13]. The emission spectrum shows a ZPL at 77760 cm^{-1} , coinciding with the ZPL in the excitation spectrum, and a dominating vibronic line at energy distance $\sim 370 \text{ cm}^{-1}$. The excitation spectrum of VUV luminescence agrees well with the $\text{Gd}^{3+} 4f^7-4f^65d$ absorption spectrum in $\text{CaF}_2:\text{Gd}^{3+}$ obtained in [14]. In addition to the structure above the edge at 77760 cm^{-1} , the excitation spectrum shows a rather rich and well-pronounced structure above ZPL at 79710 cm^{-1} .

VUV luminescence from $\text{CaF}_2:\text{Gd}^{3+}$ is observed only at low temperatures and is completely quenched near 150 K. Temperature dependence of the VUV luminescence decay curves is shown in Fig. 2. The decay kinetics is single-exponential at any temperature. The dependence of decay time on temperature was approximated by the standard formula for thermal quenching via an activation barrier E_a : $\tau = [1/\tau_r + 1/\tau_{nr} \exp(-E_a/k_B T)]^{-1}$ (shown in the inset of Fig. 2), where τ_r stands for the radiative decay time (8.5 ± 0.1 ns at 10 K) and the second term in the formula describes temperature dependence of nonradiative decay. An activation energy $E_a \sim 680 \text{ cm}^{-1}$ for thermal quenching was obtained from the fit. Thermal quenching of $\text{Gd}^{3+} 5d-4f$ luminescence is attributed to phonon assisted nonradiative relaxation (intersystem crossing) from the lowest $\text{Gd}^{3+} 5d$ level to lower-lying $4f$ levels since many $4f$ levels are located in the same energy region as the $5d$ state. The direct $5d-4f$ nonradiative transitions (at low temperature) are heavily spin-forbidden because the spin

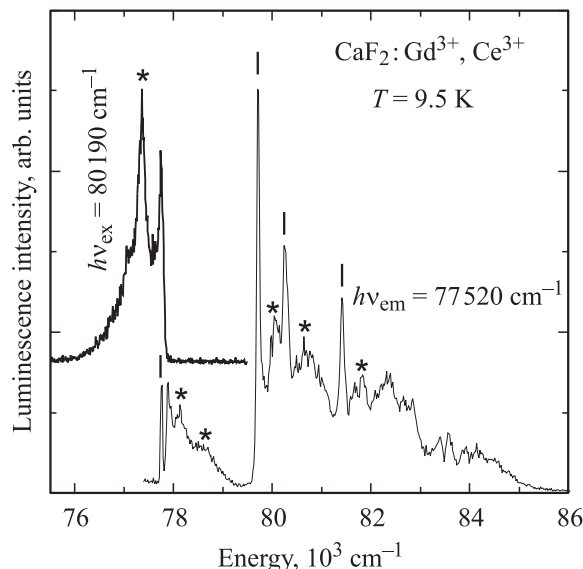


Figure 1. High-resolution ($\Delta\lambda \sim 1 \text{ \AA}$) VUV emission spectrum under 124.7 nm excitation (bold solid curve) and high-resolution ($\Delta\lambda \sim 1 \text{ \AA}$) excitation spectrum of $\text{Gd}^{3+} 4f^65d-4f^7$ emission at 129 nm (thin solid curve) from $\text{CaF}_2:\text{Gd}^{3+}$ (0.1%), Ce^{3+} (0.05%) crystal. Spectral lines tentatively ascribed to ZPLs are marked by short lines, and to dominating vibronic lines, by asterisks. $T = 9.5$ K.

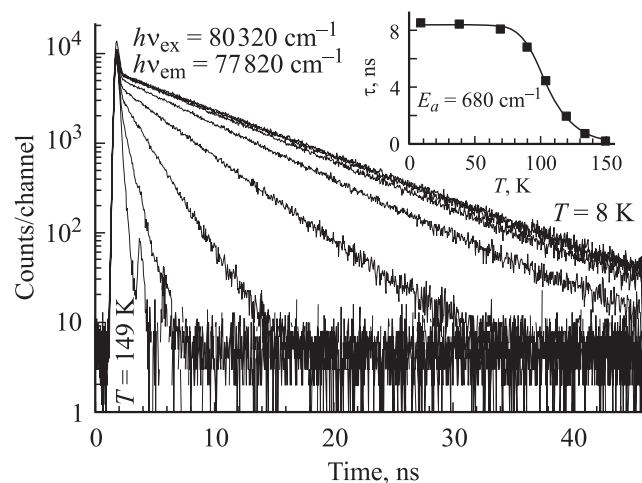


Figure 2. Temperature dependence of decay kinetics for $\text{Gd}^{3+} 4f^65d-4f^7$ emission from $\text{CaF}_2:\text{Gd}^{3+}$ (0.1%), Ce^{3+} (0.05%) crystal measured at 8, 38, 69, 89, 104, 119, 134 and 149 K. In the inset, the temperature dependence of decay time is shown (see the text for details).

multiplicity of the lowest $4f^65d$ level of Gd^{3+} is eight, whereas the $4f^7$ levels of Gd^{3+} closest to the $4f^65d$ level are spin doublets or quartets [17].

Only a slow VUV luminescence has been detected from the Lu^{3+} doped CaF_2 crystals, with a dominating peak at 79980 cm^{-1} (Figs 3, 4). This luminescence has been ascribed to $4f^{135d}-4f^{14}$ radiative transitions in Lu^{3+} . Similar to results obtained in [12] for LiLuF_4 and $\text{LiYF}_4:\text{Lu}^{3+}$,

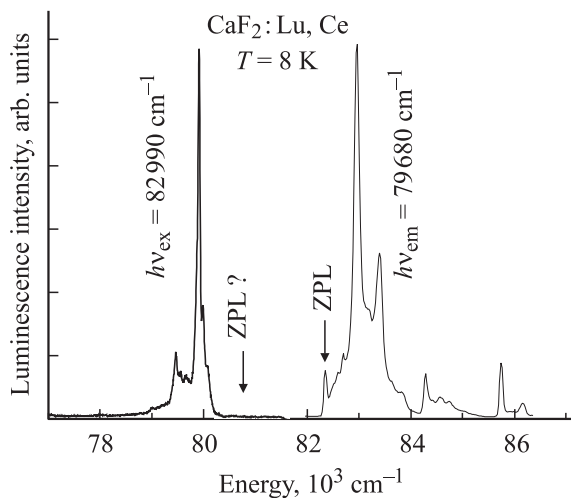


Figure 3. Lu³⁺ 4f¹³5d–4f¹⁴ emission (bold solid curve) and 4f¹⁴–4f¹³5d excitation (thin solid curve) spectra from CaF₂:Lu³⁺ (0.04%), Ce³⁺ (0.02%) crystal at T = 8 K.

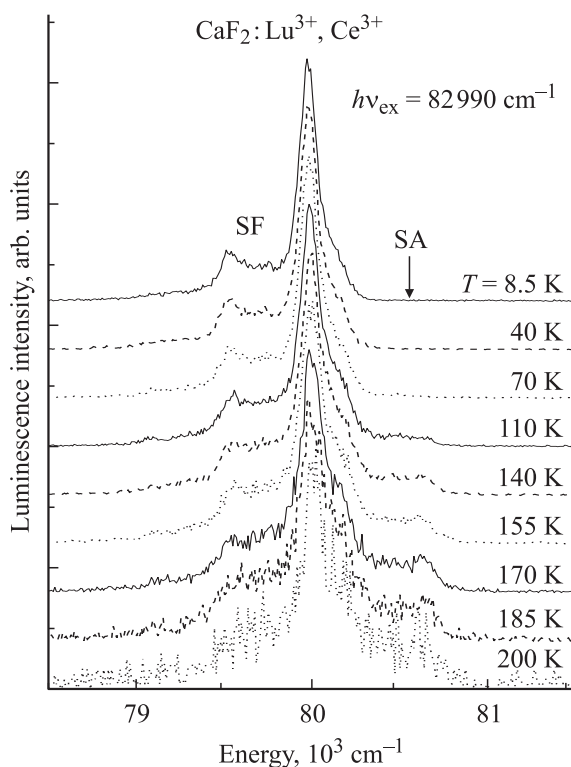


Figure 4. Normalized emission spectra from CaF₂:Lu³⁺ (0.04%), Ce³⁺ (0.02%) crystal excited by 120.5 nm photons at different temperatures (measured with moderate resolution).

only spin-forbidden (SF) 5d–4f luminescence of Lu³⁺ is observed from CaF₂:Lu³⁺ at low temperatures. However, an increase of temperature above 100 K causes appearance of an additional higher-energy emission band attributed to spin-allowed (SA) 5d–4f transitions (Fig. 4). Excitation spectra of both bands coincide and correspond to SA 4f¹⁴–4f¹³5d transitions in Lu³⁺. From the shape of

emission spectrum at T > 100 K one can estimate that the splitting between higher-lying low-spin (LS, S = 0) and lower-lying high-spin (HS, S = 1) 4f¹³5d levels of Lu³⁺ in CaF₂, from which SA and SF 5d–4f transitions take place, respectively, is less than two phonon energies. As a result, the rate of phonon nonradiative relaxation exceeds considerably that of the radiative decay for the higher-lying LS 4f¹³5d state of Lu³⁺, so that at low temperature, only SF 5d–4f luminescence from Lu³⁺ is observed. The temperature increase opens another decay channel for the lowest HS 4f¹³5d state of Lu³⁺, namely the thermal population of the higher-lying LS 4f¹³5d state, from which the 5d–4f radiative transitions are spin-allowed. However, because of „indirect“ thermal mechanism of population, the decay kinetics of SA luminescence is controlled by the slow decay of SF transitions.

At low temperature, the spectrum of VUV luminescence from CaF₂:Lu³⁺ shows no ZPL (similar to the case of LiYF₄:Lu³⁺ [12]) because purely electronic SF 4f¹³5d–4f¹⁴ transitions in Lu³⁺ are very weak (Fig. 3). The narrow lines observed in the spectrum are due to vibronics. The excitation spectrum of this emission shows ZPL at 82420 cm^{–1}, which should correspond to the edge of SA 4f¹⁴–4f¹³5d transitions in Lu³⁺. The presence of distinct vibronic structure in the spectra clearly shows that electron-lattice coupling between the 4f¹³5d electronic configuration of the Lu³⁺ ion and the lattice vibrations in CaF₂:Lu³⁺ is rather weak and large Stokes shift between emission and absorption cannot be expected.

However, there is a „Stokes shift“ of ~ 1750 cm^{–1} between experimental emission and excitation spectra obtained at T > 100 K for Lu³⁺ SA 4f–5d transitions. This fact can be explained, in principle, if one assumes that emission occurs from Lu³⁺ ions occupying the different sites (available in smaller concentration) than those responsible for 4f–5d absorption (available in larger concentration). However, for such small concentrations of Lu³⁺ as ~ 0.04 mol.%, the efficient energy transfer between different types of Lu³⁺ centers cannot be expected. On the other hand, theoretical calculations performed for 4f–5d absorption of Lu³⁺ introduced into LiYF₄ (S₄ local symmetry) have shown that absorption coefficient for the bands at the edge of Lu³⁺ 4f–5d SA transitions is much smaller (by more than an order of magnitude) than that in the region situated at ~ 1400 cm^{–1} above the edge [12]. For such small doping concentrations of Lu³⁺ as 0.04 mol.%, the lowest energy bands can be very weak and not seen in the experimental spectra. Following the approach of Ref. [18] for the prediction of the energy for the lowest 5d level of RE³⁺ in a particular host and taking into account that the energy of ZPL for the lowest 4f–5d transition of Ce³⁺ in CaF₂ is 31930 cm^{–1} (Fig. 5), the energy of the lowest Lu³⁺ LS (S = 0) 4f¹³5d level in CaF₂:Lu³⁺ is expected at ~ 81 100 cm^{–1}, which is much smaller than the energy of ZPL in excitation spectrum and much larger than the energy of the high-energy SA band in the VUV emission spectrum of CaF₂:Lu³⁺. So, additional experimental and

theoretical studies are needed in order to find out the nature of the observed unusual „Stokes shift“.

The $\text{Lu}^{3+} 5d-4f$ luminescence is almost completely quenched at temperatures $T > 200$ K. The Lu^{3+} ion has no excited $4f$ levels, and therefore thermal quenching of $\text{Lu}^{3+} 5d-4f$ luminescence cannot be due to nonradiative transitions to $4f$ levels and should be attributed to thermally activated ionization of $5d$ electrons to the conduction band. By taking into account that energy separation between the lowest $5d$ (HS) level and the bottom of the conduction band is the smallest one for Lu^{3+} among all RE ions [19], it can be expected that the $5d-4f$ luminescence from Lu^{3+} is quenched at lower temperatures than that from Er^{3+} or Tm^{3+} ($T > 500$ K [20]).

The lowest-energy band in the $\text{Ce}^{3+} 4f-5d$ excitation spectrum and $\text{Ce}^{3+} 5d-4f$ emission spectrum measured under the excitation into this lowest-energy excitation band well correspond to the spectra of Ce^{3+} center in CaF_2 in a site of tetragonal (C_{4v}) symmetry [1–3] for all singly and doubly doped CaF_2 samples studied here (Figs 5 and 6). As expected, the vibronic structure in these spectra is dominated by the line at the energy interval ~ 480 cm^{-1} from the ZPL, which well corresponds to the longitudinal optical phonon energy in CaF_2 [21], but has been usually interpreted as the local breathing mode oscillations of the eight fluorine ions surrounding the Ce^{3+} ion [22]. The excitation spectra of $\text{Ce}^{3+} 5d-4f$ emission are also very similar for all three kinds of Ce^{3+} containing samples. In addition to the excitation band corresponding to transitions to the lowest $\text{Ce}^{3+} 5d$ level (originating from the E_g band of cubic symmetry), the group of three bands in the region 180–205 nm is observed in the spectrum, which correspond to transitions to the $\text{Ce}^{3+} 5d$ states in a site of C_{4v} symmetry originating from the T_{2g} band of cubic symmetry [2]. The bands at ~ 240 nm and ~ 214 nm, also observed in the spectra of all studied samples, should belong to some other kind of Ce^{3+} centers and are usually explained as being due to absorption by Ce^{3+} clusters.

As was shown in [2], absorption spectrum of Ce^{3+} trigonal (C_{3v}) centers has a specific feature at the edge of $4f-5d$ absorption: two closely spaced (separated by ~ 30 cm^{-1}) lines corresponding to absorption from the ground $4f$ level and from the first excited $4f$ level of the $^2F_{5/2}$ ground multiplet. The latter „hot line“ appears in absorption spectrum at high enough temperature and is very weak at 15 K. However, in emission spectrum both the lines should be well seen, also at low temperature. Indeed a characteristic two-line feature can be clearly observed in $\text{Ce}^{3+} 5d-4f$ emission spectra measured from all three types of Ce^{3+} doped crystals under excitation to higher-lying than the lowest $5d$ band (Fig. 5). The energy difference ~ 135 cm^{-1} between the shortest-wavelength line in this doublet and the ZPL in the spectrum of $\text{Ce}^{3+} 5d-4f$ emission from tetragonal (C_{4v}) centers should be considered as the energy difference between the lowest $5d$ levels of Ce^{3+} ions occupying tetragonal (C_{4v}) and trigonal (C_{3v}) sites. The $4f-5d$ excitation bands of Ce^{3+} in C_{3v} sites are

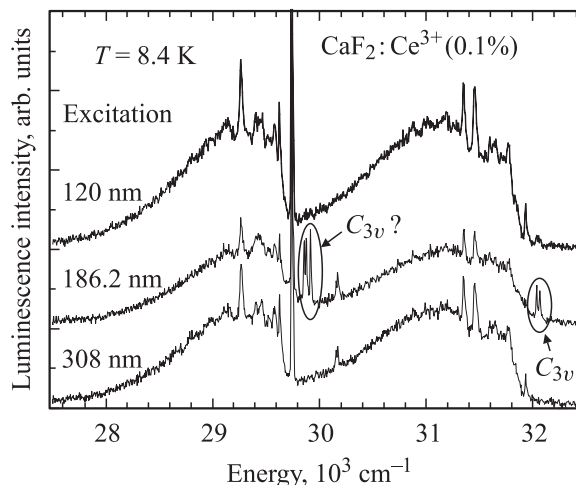


Figure 5. $\text{Ce}^{3+} 5d-4f$ emission spectrum measured from the $\text{CaF}_2:\text{Ce}^{3+}$ (0.1 mol.%) crystal under excitation to the lowest and higher-lying $\text{Ce}^{3+} 5d$ bands. $T = 8.4$ K. The features assigned to ZPLs of $5d-4f$ transitions in Ce^{3+} ions occupying trigonal (C_{3v}) sites are marked.

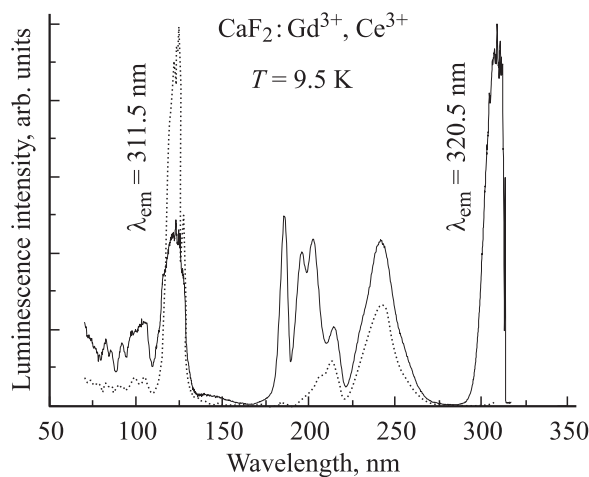


Figure 6. Excitation spectra of $\text{Gd}^{3+} 6P_{7/2}-8S_{7/2}$ emission at 311.5 nm (dotted curve) and of $\text{Ce}^{3+} 5d-4f$ emission at 320.5 nm (solid curve) from the $\text{CaF}_2:\text{Gd}^{3+}$ (0.1%), Ce^{3+} (0.05%) crystal. $T = 9.5$ K.

hidden behind the intense $4f-5d$ excitation bands of Ce^{3+} in C_{4v} sites since the concentration of the latter centers is obviously much higher.

Simultaneously with the doublet feature at the short-wavelength side of emission spectrum, another feature, consisting of three lines, appears at the short-wavelength side from ZPL corresponding to $\text{Ce}^{3+} 5d-4f$ ($^2F_{7/2}$) transitions in tetragonal (C_{4v}) centers (Fig. 5). These three lines should be assigned to transitions from the lowest $5d$ level to the lowest and two excited Stark levels of the $4f$ ($^2F_{7/2}$) multiplet of Ce^{3+} in the trigonal (C_{3v}) sites. By taking into account the 135 cm^{-1} difference between the lowest $5d$ levels of Ce^{3+} ions in tetragonal (C_{4v}) and trigonal (C_{3v}) sites, the lowest level of the $4f$ ($^2F_{7/2}$)

multiplet should have lower energy (by $\sim 45 \text{ cm}^{-1}$) for the trigonal (C_{3v}) site than for the tetragonal (C_{4v}) site.

As it is clearly seen in Fig. 6, Gd³⁺ ${}^6P_{7/2}$ – ${}^6S_{7/2}$ emission at $\sim 311 \text{ nm}$ is not excited in the CaF₂:Gd³⁺, Ce³⁺ crystal under the excitation to the lowest-energy Ce³⁺ 5d band as well as to the group of three bands in the region 180–205 nm, all corresponding to transitions to the Ce³⁺ 5d levels in a site of tetragonal (C_{4v}) symmetry. Thus, absorption of photon by the Ce³⁺ ion in a tetragonal site results in fast relaxation of energy to the lowest Ce³⁺ 5d level from which the characteristic Ce³⁺ 5d–4f emission is observed. No energy transfer to Gd³⁺ is observed in this case because the energy of the lowest 5d level of Ce³⁺ in a site of tetragonal symmetry is lower than the energy of the Gd³⁺ 4f(${}^6P_{7/2}$) level. The Gd³⁺ 311 nm emission is well excited in the region of 240 and 213 nm excitation bands, which were assigned to 4f–5d transitions in Ce³⁺ clusters. This occurs because the energy of the lowest 5d level of Ce³⁺ in such centers is higher or nearly the same as the energy of the Gd³⁺ 4f(${}^6P_{7/2}$) level. Accordingly, the energy transfer can take place from these Ce³⁺ centers to Gd³⁺.

Although theoretical calculations of interconfigurational transitions in Gd³⁺ and Lu³⁺ ions doped into CaF₂ are not available, some narrow lines in the spectra can be tentatively ascribed to ZPLs accompanied by some vibronic structure. Such a simplified analysis allows anyway to make a conclusion that the fine structure in the emission and excitation spectra of interconfigurational transitions in these ions is definitely not dominated by the vibronic lines at the energy interval $\sim 480 \text{ cm}^{-1}$ from ZPLs. This indicates that Gd³⁺ and Lu³⁺ ions reside in CaF₂ predominantly in sites of different type than of tetragonal (C_{4v}) symmetry. The main features of vibronic structure in Gd³⁺ 4f⁶5d–4f⁷ emission spectrum and in the lowest-energy band of Gd³⁺ 4f⁷–4f⁶5d excitation spectrum are separated by $\sim 370 \text{ cm}^{-1}$ from ZPLs. This energy does not correspond to any well-defined peaks in phonon spectrum of CaF₂, and some pseudo-local modes should be involved in electron-lattice coupling between the 4f⁶5d electronic configuration of the Gd³⁺ ion and the lattice vibrations in CaF₂. The analysis of vibronic structure in the spectra of interconfigurational transitions in Lu³⁺ is even more complicated since ZPL is not observed in the spectrum of Lu³⁺ SF 4f¹³5d–4f¹⁴ luminescence.

Conclusions

By using the high-resolution VUV spectroscopy technique, the Lu³⁺ 4f¹³5d–4f¹⁴ luminescence from the CaF₂:Lu³⁺, Ce³⁺ crystal has been detected, assigned and characterized. The measurements of emission spectra under spectrally selective excitation from CaF₂ doubly doped with Gd³⁺ and Ce³⁺ or Lu³⁺ and Ce³⁺ as well as singly doped with Ce³⁺ have confirmed that for doping concentrations below $\sim 0.1 \text{ mol.}\%$, the Ce³⁺ ions reside in CaF₂ pre-

dominantly in the tetragonal (C_{4v}) sites. However, the presence of Ce³⁺ trigonal (C_{3v}) centers was also detected and several lines in emission spectra were assigned to ZPLs corresponding to 5d–4f transitions in Ce³⁺ entering the trigonal (C_{3v}) sites. The vibronic structure in the emission and excitation spectra of interconfigurational transitions in Gd³⁺ and Lu³⁺ ions in CaF₂ differs from that observed for Ce³⁺ ions at the tetragonal (C_{4v}) sites. However, the types of sites in which the Gd³⁺ and Lu³⁺ ions reside in the CaF₂ lattice cannot be identified basing only on experimental spectroscopic data available.

The authors would like to thank Prof. G. Zimmerer and Prof. B.Z. Malkin for valuable discussions.

References

- [1] A.A. Kaplyanskii, V.N. Medvedev, P.P. Feofilov. Opt. Spektrosk. **14**, 644 (1963).
- [2] W.J. Manthey. Phys. Rev. B **8**, 4086 (1973).
- [3] T. Szczurek, M. Schlesinger. In: Rare earth spectroscopy / Eds B. Jezowska-Trebatowska, J. Legendziewich, W. Strek. World Scientific, Singapore (1985). P.309.
- [4] Y.K. Voron'ko, A.A. Kaminskii, V.V. Osiko. JETP **50**, 15 (1966).
- [5] I.T. Jacobs, G.D. Jones, K. Zdansky, R.A. Satten, Phys. Rev. B **3**, 2888 (1971).
- [6] M. Yamaga, S. Yabashi, Y. Masui, M. Honda, H. Takahashi, M. Sakai, N. Sarukura. J.-P.R. Wells, G.D Jones. J. Lumin. **108**, 307 (2004).
- [7] P.W. Pack, W.J. Manthey, D.S. McClure. Phys. Rev. B **40**, 9930 (1989).
- [8] S.P. Jamison, R.J. Reeves, P.P. Pavlichuk, G.D. Jones. J. Lumin. **83-84**, 429 (1999).
- [9] M. Kirm, J.C. Krupa, V.N. Makhov, M. True, S. Vielhauer, G. Zimmerer, Phys. Rev. B **70**, 241 101(R) (2004).
- [10] M. Kirm, V.N. Makhov, M. True, S. Vielhauer, G. Zimmerer. Fiz. Tverd. Tela **47**, 1368 (2005).
- [11] V.N. Makhov, J.C. Krupa, M. Kirm, G. Stryganyuk, S. Vielhauer, G. Zimmerer. Izv. Vuzov, ser. Fiz. **4** (Suppl.), 86 (2006).
- [12] M. Kirm, G. Stryganyuk, S. Vielhauer, G. Zimmerer, V.N. Makhov, B.Z. Malkin, O.V. Solovyev, R.Yu. Abdulsabirov, S.L. Korableva. Phys. Rev. B **75**, 075 111 (2007).
- [13] V.N. Makhov, S.Kh. Batygov, L.N. Dmitruk, M. Kirm, G. Stryganyuk, and G. G. Zimmerer. Phys. Status. Solidi C **4**, 881 (2007).
- [14] M. Schlesinger, T. Szczurek, G.W.F. Drake. Solid State Commun. **28**, 165 (1978).
- [15] G. Zimmerer. Nucl. Instrum. Meth. A **308**, 178 (1991).
- [16] G. Zimmerer. Rad. Measurements, **42**, 859 (2007).
- [17] P.S. Peijzel, A. Meijerink, R.T. Wegh, M.F. Reid, G.W. Burdick. J. Solid State Chem. **178**, 448 (2005).
- [18] P. Dorenbos. J. Lumin. **91**, 91, (2000).
- [19] P. Dorenbos. J. Phys.: Cond. Matter **15**, 8417 (2003).
- [20] V.N. Makhov, T. Adamberg, M. Kirm, S. Vielhauer, G. Stryganyuk. J. Lumin., **128**, 725 (2008).
- [21] R.P. Lowndes. J. Phys. C: Solid State Phys. **4**, 3083 (1971).
- [22] W. Hayes, M.C.K. Wiltshire, W.J. Manthey, D.S. McClure. J. Phys. C: Solid State Phys. **6**, L273 (1973).